Saudi Pharmaceutical Journal 28 (2020) 147–154

Contents lists available at ScienceDirect

Saudi Pharmaceutical Journal

journal homepage: www.sciencedirect.com

Original article

Toxicity evaluation of 6-mercaptopurine-Chitosan nanoparticles in rats

Prem Kumar Govindappa [a,b,*], Darukeshwara Joladarashi [c], Raghavendra Lakshmana Shetty Hallur [d], Jagadeesh S. Sanganal [b], Ayyalasomayajula Ratna Phani [e]

[a] Department of Orthopaedics and Rehabilitation, College of Medicine, The Pennsylvania State University, Hershey, PA 17033, USA
[b] Department of Veterinary Pharmacology and Toxicology, Veterinary College, Hebbal, Bangalore, Karnataka 560 024, India
[c] Department of Molecular Pharmacology and Physiology, Morsani College of Medicine, University of South Florida, Tampa, FL 33613, USA
[d] Department of Gynecology and Obstetrics, Botucatu Medical School (FMB), São Paulo State University (UNESP), CEP18618-687 São Paulo, Brazil
[e] Innovative Nano and Micro Technologies Private Limited, Mysore Road, Bangalore, Karnataka 5600059, India

ARTICLE INFO

Article history:
Received 24 July 2019
Accepted 29 November 2019
Available online 7 December 2019

Keywords:
6-Mercaptopurine
Chitosan
Nanoparticle
Anti-cancer
Toxicity

ABSTRACT

Background: The 6-mercaptopurine (6-MP) is an effective immunosuppressant and anti-cancer drug. However, the usage of 6-MP is limited due to its well-known side effects, such as myelotoxicity and hepato-renal toxicity. To curtail the potential toxic effects, we have used chitosan as a natural biodegradable and biocompatible polysaccharide to synthesize 6-Mercaptopurine-Chitosan Nanoparticles (6-MP-CNPs).
Methods: The 6-MP-CNPssize, morphology, physicochemical interactions, and thermal stability were characterized using Dynamic Light Scattering (DLS), Scanning Electron Microscopy (SEM), Fourier Transform Infrared Spectroscopy (FTIR), and Differential Scanning Calorimetry (DSC), respectively. The loading efficiency of the 6-MP in CNPs was estimated using LCMS/MS. Then, the 6-MP-CNPs were subjected to *in vivo* acute and sub-acute oral toxicity evaluations.
Results: The DLS and SEM analysis respectively indicated size (70.0 nm to 400.0 nm), polydispersity index (0.462), and zeta potential (54.9 mV) with improved morphology of 6-MP-CNPs. The FTIR and DSC results showed the efficient interactive and stable nature of the 6-MP-CNPs, which sustained the drug-delivery process. The loading efficiency of 6-MP-CNPs was found to be 25.23%. The chitosan improved the lethal dose (LD50 cut off) of 6-MP-CNPs (1000 mg/kg b.w) against 6-MP (500 mg/kg b.w) and also significantly ($p \leq 0.05$) reduces the toxic adverse effect (28-day repeated oral dose) on hemato-biochemical and hepato-renal histological profiles.
Conclusion: The findings suggest that chitosan, as a prime drug-delivery carrier, significantly alleviates the acute and sub-acute toxic effects of 6-MP.

1. Introduction

The 6-mercaptopurine (6-MP) is an effective immunosuppressant and anti-cancer agent. The agent is increasingly prescribed in human and veterinary medicine to treat inflammatory (Crohn's syndrome, ulcerative colitis, rheumatologic disorders, *etc.*) and leukemia (acute lymphoblastic leukemia and acute myelocytic leukemia) conditions (Fotoohi et al., 2010; Lennard et al., 1993). However, the metabolites [6-thioguanine (6-TGN) and 6-methylmercaptopurine (6-MM)] of 6-MP at short- and long-term therapeutic conditions accumulate in the cells to cause myeloid, renal, and hepatic toxicities without much survival benefit (Adam de Beaumais et al., 2011; Vora et al., 2006). Although the specification mode of 6-MP is not fully understood, its cytotoxicity and immunosuppressive activities have been linked to the incorporation of its metabolite, 6-TGN/6-MM, into the DNA resulting in impaired DNA synthesis and cell death (Benkov et al., 2013; Coelho et al., 2016).

There are different methods of preparing chitosan nanoparticles, which include, emulsion droplet coalescence (Tokumitsu et al., 1999), emulsification and cross-linking (Songjiang and Lixiang, 2009), emulsion solvent diffusion (El-Shabouri, 2002),

* Corresponding author at: Department of Orthopaedics and Rehabilitation, The Pennsylvania State University College of Medicine, 500 University Drive, Mail Code H089, Hershey, PA 17033, USA.
E-mail address: drpremkamal@gmail.com (P.K. Govindappa).
Peer review under responsibility of King Saud University.

Production and hosting by Elsevier

https://doi.org/10.1016/j.jsps.2019.11.018
1319-0164/

reverse micellization (Tang et al., 2007), ionic gelation (Kumar et al., 2015), polyelectrolyte complexation (Yeh et al., 2011), modified ionic gelation with radical polymerization (Sajeesh and Sharma, 2006), and desolvation (Atyabi et al., 2009). Among these methods, the ionic gelation technique has received much attention due to it's non-toxic, convenient, and controllable process (Agnihotri et al., 2004).

Chitosan [poly β (1, 4) 2-amino-2-deoxy-D-glucose] is a natural biocompatible polymer with excellent encapsulation efficiencies and sustained release properties, ensuring efficiency in the drug-delivery system (Mohammed et al., 2017). Being a cationic polysaccharide, chitosan interacts with sodium tripolyphosphate (TPP) by electrostatic forces (Shu and Zhu, 2002). This important cross-linking mechanism not only helps to encapsulate target drugs/biological samples but also avoids the use of harsh chemicals for cross-linking and emulsifying processes, which are often toxic to organisms (Berger et al., 2004).

In this study, we have used chitosan as a natural polysaccharide to reduce the potential side effects of 6-mercaptopurine nanoparticles. The 6-mercaptopurine-chitosan nanoparticles (6-MP-CNPs) were synthesized, characterized, and evaluated for their effects on the hematological, biochemical, and hepato-renal histopathological changes in the toxicity studies.

2. Materials and methods

2.1. Materials

The 6-mercaptopurine monohydrate (assay purity98.0%), chitosan low-molecular-weight (deacetylation ≥ 75.0%), TPP (purity: 85%), glacial acetic acid (≥99.85%), and dimethylformamide (DMF) were purchased from Sigma-Aldrich.

2.2. Methods

2.2.1. Synthesis of 6-MP-CNPs

The 6-MP-CNPs were synthesized by the ionic gelation technique using chitosan and TPP as described in the literature with slight modification (Gan and Wang, 2007; Kumar et al., 2015). Briefly, a known concentration of chitosan was dissolved in 1% (v/v) acetic acid and mixed with the 6-MP solution (1 mg/mL of DMF). Tween 80 (0.5% v/v) was added to the chitosan solutions, and pH was maintained at ~4.5. The 6-MPcontaining chitosan solutions was then stirred with TPP solution (2:1 v/v) for 30 min and centrifuged at 10,000g for 30 min. The pellet was resuspended with Milli-Q-water and freeze-dried in a vacuum (ScanVacCoolSafe Freeze Drying, CoolSafe 110-4).

2.2.2. Characterization of nanoparticles

2.2.2.1. Dynamic Light Scattering (DLS) and Scanning Electron Microscopy (SEM). The size and surface morphology of 6-MP-CNPs were determined using DLS (ZetasizerNano ZS90, Malvern, UK) and SEM (XL 30, Philips, Eindhoven, The Netherlands), respectively. Nanoparticles were sputter-coated with gold (SCD005; Bal-tec, Balzers, Liechtenstein) before SEM observation. The nanoparticles'stability and surface charge were analyzed by zeta potential measurements (ZetasizerNanoZS90, Malvern, UK) using fold capillary cuvette (Folded Capillary Cell-DTS1060, Malvern, UK).

2.2.2.2. Fourier Transform Infrared Spectroscopy (FTIR) analysis. The FTIR procedure involving sample preparations and spectral recordings were carried out by a previously described method (Moll, 1971). The IR spectra of 6-MP, chitosan nanoparticles (CNPs), and 6-MP-CNPs were recorded using FTIR Bruker optics, alpha, and operated by OPUS Spectroscopy Software. The formulations were individually placed on the sample plate of the smart orbit and lightly screwed to record the IR spectra in ATR mode.

2.2.2.3. Differential Scanning Calorimetry (DSC). The DSC analysis of 6-MP and 6-MP-CNPs were performed using Auto Q20 V24.10 DSC instrument (Universal V4.5A TA Instruments). The initial and final temperatures ranged from 0 °C to 350 °C at a heating rate of 10 °C min^{-1}. Nitrogen gas (99.99% purity) atmosphere was utilized in all the cases, and the instrument was calibrated using indium as the reference material.

2.2.3. Swelling behavior study

To understand the swelling nature, CNPs were incubated in 25 mL normal saline (0.9% NaCl) at ambient temperature for 48 h. After incubation, the CNPs were processed and examined under SEM.

2.2.4. The 6-MP loading efficiency of CNPs

The 6-MP-CNPs were dissolved in methanol:water (50:50 v/v) using an ultrasonic bath sonicator for 15 min. The concentration of 6-MP was analyzed using LCMS/MS [MDS SCIEX Q-TRAP API 3200 mass spectrometer (Foster City, CA, USA) and Agilent HPLC system]. The 6-MP standards (1 to 100 ng/mL) were prepared for the analysis of samples by plotting a straight-line graph (R^2 = 0.9997). The drug loading rate (%) was determined using below equation.

$$\text{Drug Loading } (\%) = \text{Weight of 6 - mercaptopurine} / \text{Weight of Nanoparticles} \times 100$$

2.2.5. In vivo toxicity studies

2.2.5.1. Animals. Healthy eight- to ten-week-old Wistar rats of both sexes weighing around 200 ± 20 g were procured from the Laboratory AnimalFacility, Veterinary College, Bangalore, India. The study was carried out at the Rodent Experiment Facility, Veterinary College, Bangalore, India. Animal care and usage requirements were followed based on guidelines of the NIH Publication, National Research Council (US) Committee for the Update of the Guide for the Care and Use of Laboratory Animals (2011). The Institutional Animal Ethics Committee (IAEC) approved the experimental protocol No. 139/LPM/IAEC/2013.

2.2.5.2. Acute oral toxicity study. The acute oral toxicity evaluation of the test items (6-MP and 6-MP-CNPs) was conducted in accordance with the Organization for Economic Cooperation and Development Guideline 423 (Acute toxic class method, OECD, 2001). The experimental animals (n = 3) were fasted overnight (~12 h), and the test substance was administered in a single dose (300 mg/kg b.w) by oral gavage. The animals were individually observed after dosing at least once during the first 30 min periodically for the first 24 h. Special attention was given during the first 4 h and daily after that for a total of 14 days. The LD50 cut-off (mg/kg b.w) of test items were reported, based on mortality and necropsy findings.

2.2.5.3. Sub-acute (28-day repeated dose)oral toxicity study. The sub-acute oral toxicity evaluation of the test items (6-MP and 6-MP-CNPs) was carried out in accordance with the Organization for Economic Cooperation and Development Guideline 407 (Repeated dose 28-day oral toxicity study in rodents, OECD, 2008). The experimental animals [12 animals (6 male and 6 female) per group] were randomly assigned to normal control (normal saline-2 mL/kg), 6-MP-CNPs (15 mg/kg-low dose, 30 mg/kg-mid dose, and 50 mg/kg-high dose), and 6-MP (50 mg/kg) treatment groups. These doses were selected based on the animal

equivalent dose of human dose (1 to 5 mg/kg), which are prescribed for different disease conditions (acute lymphatic leukemia, Crohn'sdisease, rheumatologic disorders, *etc*). Also, with interest to evaluate the marginal safety of 6-MP-CNPs, the selected low, mid, and high dose corresponded to therapeutic, supra-therapeutic, and toxic dose (~3 times more than therapeutic dose), respectively. All the test items were orally administered each day for 28 days, and the animals were monitored for clinical signs of toxicity.

2.2.5.4. Hematological and biochemical analysis. On day 28, the experimental animals were fasted overnight. Their blood samples were collected in anticoagulant (Calcium Disodium EDTA, Merck, India) and non-anticoagulant tubes via retro-orbital plexus using hematocrit capillary tubes under isoflurane anesthesia. Anticoagulant blood samples were immediately processed for hematological evaluations using automatic blood cell counter (ERMA PCE-210N), whereas harvested serum samples were stored at −80 °C until analysis of biochemical parameters using ErbaChem 5 Plus V2 Biochemistry Analyzer.

2.2.5.5. Histopathological analysis. After collecting the blood on day 28, the experimental animals were subjected to whole-body perfusion (Phosphate-buffered saline-PBS) and fixation (10% neutral buffered formaldehyde -NBF) to harvest their liver and kidneys. The harvested samples were stored in 10% NBF, dehydrated in graded anhydrous ethanol, and embedded in paraffin. The fine tissue sections of ~5 μm thickness were stained with hematoxylin and eosin (H&E) and examined under an Olympus BX50 light microscope.

2.2.6. Statistical analysis

The data were analyzed using a two-tailed student's *t*-test and two-way analysis of variance (ANOVA). All the values were presented as mean ± SEM. The probability (p) values of ≤0.05 were considered statistically significant.

3. Results and discussion

3.1. Synthesis and characterization of 6-MP-CNPs

The synthesis of 6-MP-CNPs was optimized using the ionic gelation technique with a constant volume ratio of chitosan: TPP (2:1) at different concentrations (Kumar et al., 2015). The most reproducible size, shape, and loading efficiency of the nanoparticles were obtained at concentrations of chitosan (0.75 mg/mL), TPP (0.5 mg/mL), and 6-MP (1.0 mg/mL). The DLS results of 6-MP-CNPs showed an average particle size (187.0 nm) with a polydispersity index (0.462) and zeta-potential (54.9 mV), which represents uniform distribution and stable nature of nanoparticles (Fig. 1A and B) (Debnath et al., 2018). The SEM image analysis of 6-MP displayed an irregular size (~10 to 40 μm) and morphology (Fig. 1C). However, the interactive nature of positively charged primary amino groups of chitosan and the negatively charged polyanion groups of TPP modified the size (~150 to 400 nm) and shape of the 6-MP (Fig. 1D) (Shu and Zhu, 2002). The synthesized CNPs were incubated for 48 hr in normal saline to understand the *in vitro* swelling behavioral properties and drug release process (Walke et al., 2015). As a result, the SEM image analysis demonstrated an increased size from ~25 to 55 nm to ~400 to 600 nm (Fig. 1E and F). To perform an *in vivo* acute and subacute toxicity studies, the loading efficiency of 6-MP-CNPs (25.23%) was quantified using LCMS/MS.

FTIR analysis was performed to determine the 6-MP and CNPs interactions. The fundamental vibrations of primary functional groups and the frequency (cm^{-1}) of the CNPs and 6-MP-CNPs are depicted in Fig. 2A and B, respectively. The stretching vibrations of —OH and C—H bond of the CNPs were observed to be 3421.92 cm^{-1} and 2935.43 cm^{-1}, respectively (Dorniani et al., 2013; Peniche et al., 1999). The absorption peaks at 1642.23 cm^{-1}, 1536.57 cm^{-1}, 1416.54 cm^{-1}, and 1385.84 cm^{-1} were assigned to C═O stretching of the amide I band, bending vibrations of the N—H (N-acetylated residues, amide II band), C—H bending, and OH bending, respectively. The peak at

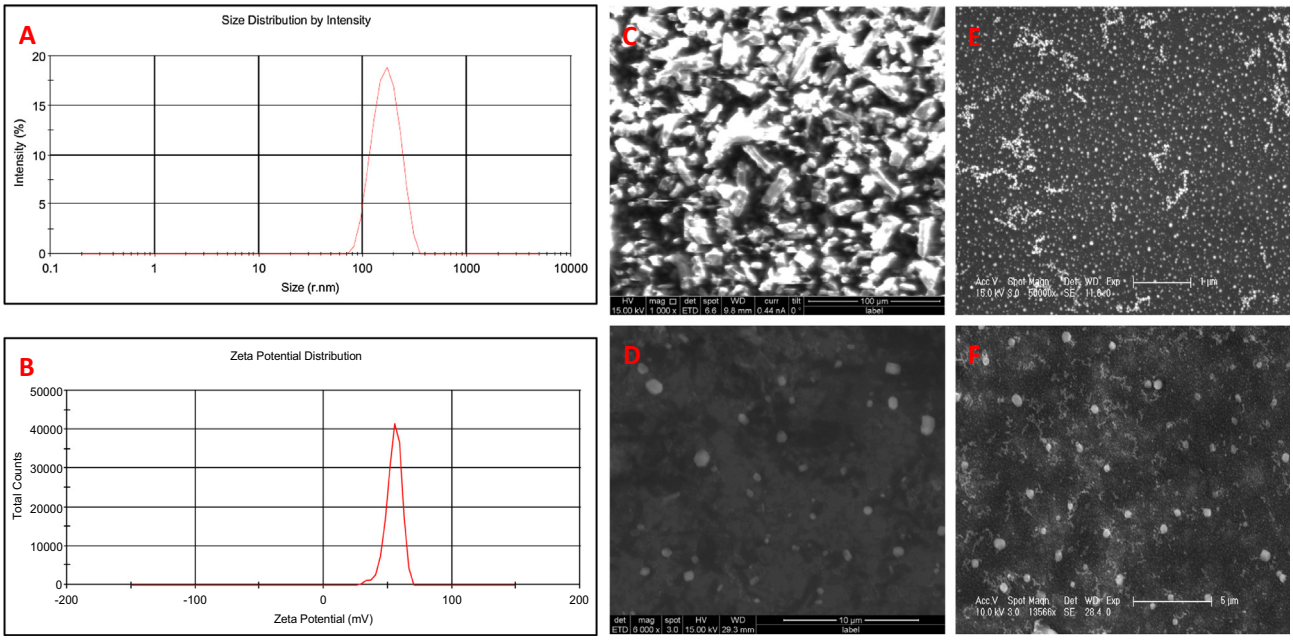

Fig. 1. DLS results of 6-MP-CNPs are depicting size distribution (A) and zeta potential distribution (B). SEM analysis of 6-MP (C), 6-MP-CNPs (D), CNPs-before swelling (E), and CNPs-after swelling (F) behavior analysis.

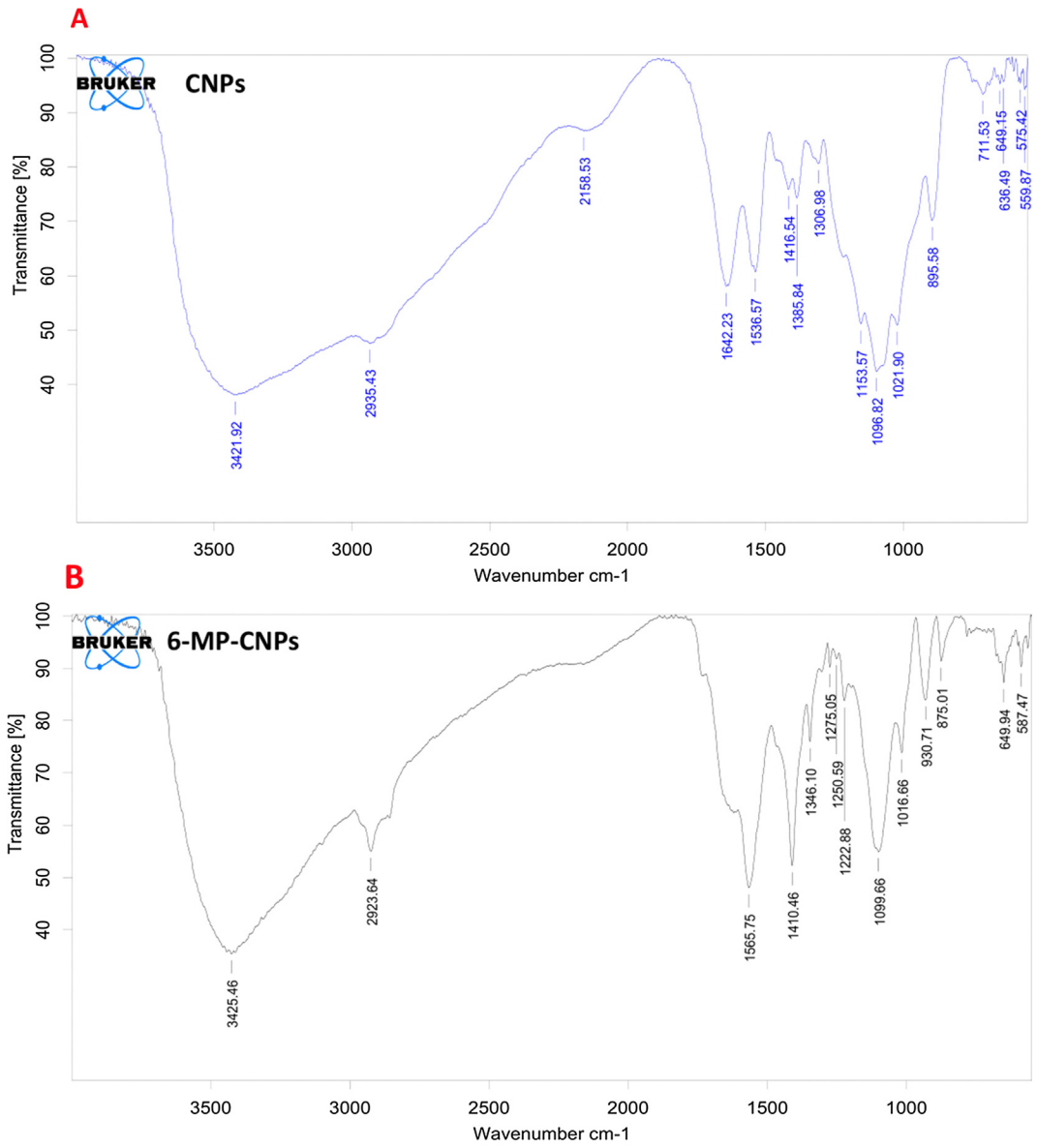

Fig. 2. FTIR results of CNPs (A) and 6-MP-CNPs (B).

1153.57 cm^{-1} was assigned to the structure of saccharide, whereas 1096.82 cm^{-1} and 1021.90 cm^{-1} were assigned to the skeletal vibrations involving the C—O stretching (Xu and Du, 2003). The peak observed in Fig. 2B for 6-MP-CNPs at 3425.46 cm^{-1} and 2923.64 cm^{-1} were assigned to N—H and C—H stretching, respectively, which confirms the 6-MP complex with CNPs. Increased intensity and shifting of peaks at 1565.75 cm^{-1} and 1410.46 cm^{-1} of the CNPs were probably due to existing adsorption and/or encapsulation process of 6-MP and CNPs, which in turn, helped to enhance the dissolution properties of 6-MP-CNPs (Kumar et al., 2014). In other words, the decrease in intensity of the peak at 1099.66 cm^{-1} (C═S/ring vibration) shown in Fig. 2B also suggests that an exocyclic (S) atom contributed with chitosan to elucidate the adsorption and/or encapsulation process of 6-MP with CNPs (Dorniani et al., 2013).

The DSC analysis was performed to assess the thermal behavior of the CNPs, 6-MP, and 6-MP-CNPs (Fig. 3A, B, and C). The CNPs exhibited a broad endothermic peak centered at 80.95 °C. This peak is attributed to the loss of water connected with the hydrophilic groups of the CNPs. The exothermic peak, which appeared at ~270 °C, corresponds to the decomposition of amine units of CNPs. We did not record the comprehensive decomposition spectrum. However, the results of Ferrero and Periolatto (2012) and Tamer et al. (2017) support our findings. The 6-MP exhibited a broad endothermic and a narrow exothermic peak centered at 183.34 °C and 211.17 °C, respectively (Lv et al., 2016). Also, thermograms of 6-MP-CNPs exhibited a reduced endothermic peak (as compared to 6-MP) centered at 143.16 °C, and a similar exothermic peak of chitosan centered at 302 °C. These minor changes are partially attributed to improved dissolution properties of 6-MP at the temperatures below its melting point. Finally, the observed peak of 6-MP in the DSC thermograms of 6-MP-CNPs was owing to the non-interactive nature of the 6-MP and chitosan polymer.

3.2. In vivo toxicity studies

3.2.1. Acute oral toxicity

Acute oral toxicity study of 6-MP-CNPs and 6-MP was started at a dose of 300 mg/kg bw. On day 14 of the experimental period, 6-MP-CNPs did not show any mortalities, although one animal died

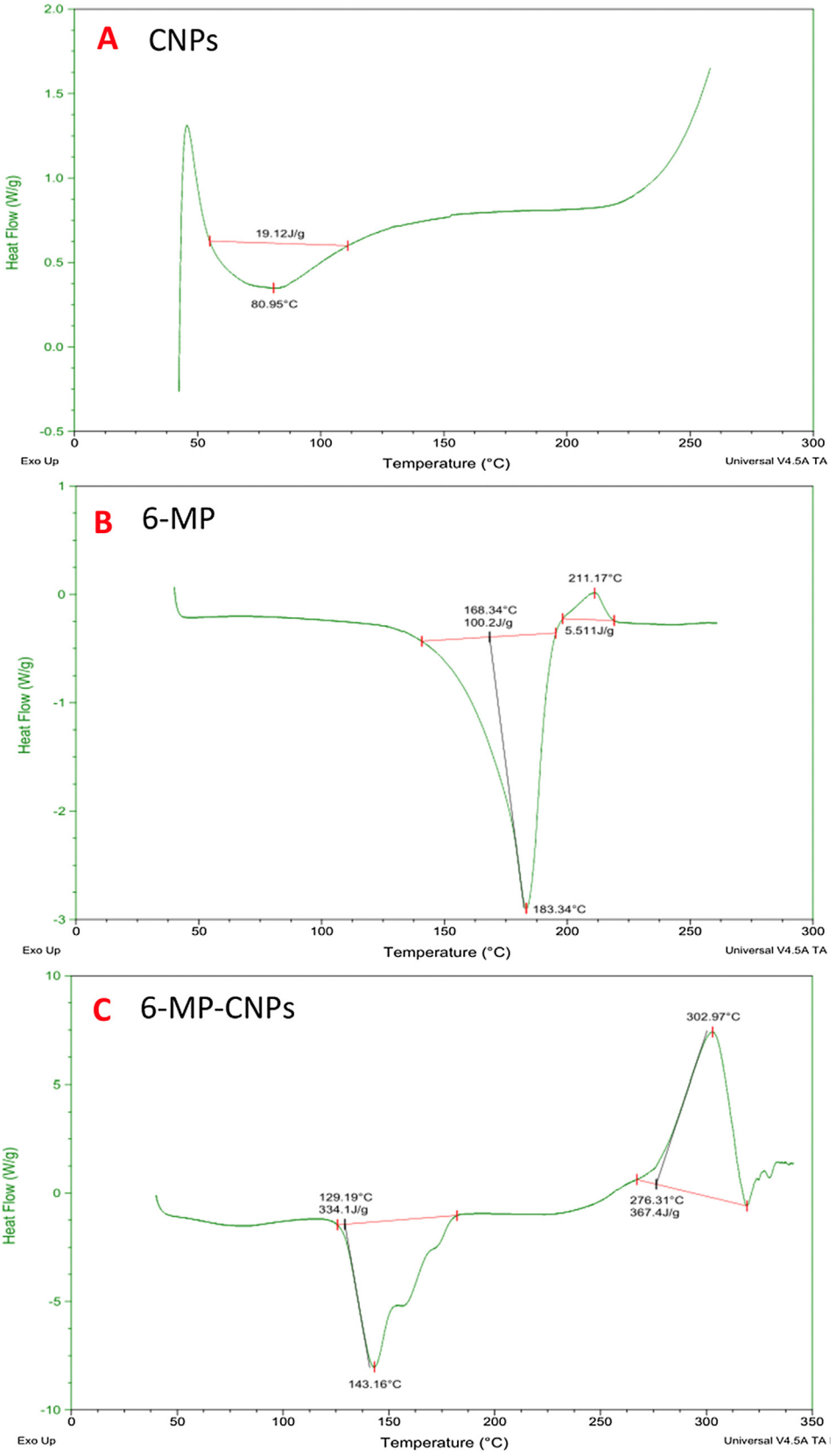

Fig. 3. DSC results of CNPs (A), 6-MP (B) and 6-MP-CNPs (C).

in the 6-MP group. Therefore, the dosing of three additional animals (with the same dose) was performed to confirm the mortality/survivability. The observed results were the same. Hence, dosing of three additional animals at the next higher dose (2000 mg/kg bw) was performed, and the resulting animal mortalities were two and three, respectively. No abnormalities were

Table 1
Hematological and biochemical results of rat blood samplesafter 28-day repeated oral dosing of saline (2 mL/kg), 6-MP (50 mg/kg), and 6-MP-CNPs (low dose-15 mg/kg, mid dose-30 mg/kg, and high dose-50 mg/kg), (n = 6, $^{ab}p < 0.001$).

Parameters	Saline (Control)	6-MP-CNPs (Low dose)	6-MP-CNPs (Mid dose)	6-MP-CNPs (High dose)	6-MP (High dose)
Male					
TEC (10^6 Cells/mm^3)	8.57 ± 0.03	7.58 ± 0.05^{ab}	7.22 ± 0.05^{ab}	4.51 ± 0.04^{ab}	3.75 ± 0.05^{a}
TLC (10^3 Cells/mm^3)	10.34 ± 0.13	9.50 ± 0.09^{ab}	9.00 ± 0.02^{ab}	6.09 ± 0.14^{ab}	4.27 ± 0.03^{a}
PCV (%)	37.97 ± 0.34	33.94 ± 1.19^{ab}	32.62 ± 1.08^{ab}	24.08 ± 0.39^{ab}	20.73 ± 0.18^{a}
Hg (g/dL)	12.34 ± 0.13	11.40 ± 0.12^{ab}	10.61 ± 0.10^{ab}	8.52 ± 0.14^{ab}	6.27 ± 0.03^{a}
ALT (U/L)	33.33 ± 0.20	49.41 ± 1.26^{ab}	56.74 ± 2.27^{ab}	88.29 ± 2.21^{ab}	100.48 ± 2.29^{a}
AST (U/L)	60.96 ± 0.30	84.37 ± 1.24^{ab}	97.94 ± 2.32^{ab}	124.29 ± 1.24^{ab}	150.13 ± 1.45^{a}
ALP (U/L)	63.49 ± 0.02	76.39 ± 2.44^{ab}	88.90 ± 2.23^{ab}	133.97 ± 1.23^{ab}	168.44 ± 2.20^{a}
Creatinine (mg/dL)	0.75 ± 0.01	0.95 ± 0.04^{ab}	1.16 ± 0.01^{ab}	1.36 ± 0.01^{ab}	1.84 ± 0.01^{a}
BUN (U/L)	21.93 ± 0.30	24.04 ± 1.24^{ab}	26.23 ± 1.12^{ab}	36.16 ± 0.19^{ab}	45.68 ± 0.26^{a}
Female					
TEC (10^6 Cells/mm^3)	8.50 ± 0.01	7.52 ± 0.04^{ab}	7.20 ± 0.04^{ab}	4.46 ± 0.03^{ab}	3.69 ± 0.04^{a}
TLC (10^3 Cells/mm^3)	10.08 ± 0.02	9.15 ± 0.03^{ab}	8.86 ± 0.06^{ab}	5.52 ± 0.14^{ab}	4.25 ± 0.02^{a}
PCV (%)	37.08 ± 0.34	33.94 ± 1.99^{ab}	32.73 ± 1.80^{ab}	24.08 ± 0.39^{ab}	20.73 ± 0.18^{a}
Hg (g/dL)	11.34 ± 0.13	10.47 ± 0.10^{ab}	9.73 ± 0.06^{ab}	7.52 ± 0.14^{ab}	5.27 ± 0.03^{a}
ALT (U/L)	32.05 ± 0.51	46.03 ± 0.65^{ab}	54.04 ± 0.30^{ab}	86.34 ± 2.54^{ab}	106.81 ± 4.20^{a}
AST (U/L)	60.05 ± 2.40	84.13 ± 2.13^{ab}	91.59 ± 3.16^{ab}	128.97 ± 2.30^{ab}	151.85 ± 2.13^{a}
ALP (U/L)	62.14 ± 1.29	80.33 ± 3.84^{ab}	86.09 ± 3.23^{ab}	131.31 ± 2.35^{ab}	156.44 ± 3.47^{a}
Creatinine (mg/dL)	0.75 ± 0.01	0.84 ± 0.01^{ab}	0.97 ± 0.08^{ab}	1.29 ± 0.01^{ab}	1.64 ± 0.01^{a}
BUN (U/L)	20.82 ± 0.26	22.98 ± 1.14^{ab}	25.79 ± 2.30^{ab}	34.72 ± 0.25^{ab}	43.26 ± 0.25^{a}

found in the organs at necropsy. The toxicity of 6-MP-CNPs and 6-MP in Globally Harmonized Classification System (GHS) was categorized as Category 4 (>300–2000 mg/kg bw). Hence, the respective LD_{50} cut-off values were1000 and 500 mg/kg bw (Clarke et al., 1953). Therefore, a lethal dose of 6-MP-CNPswas considerably more than 6-MP.

3.2.2. Sub-acute oral toxicity

3.2.2.1. Hematological and biochemical parameters. The high dose of 6-MP and 6-MP-CNPs treatment (for either sex) indicated significant ($^{ab}p < 0.001$) reduction in the hematological parameters [total erythrocyte count (TEC), total leucocyte count (TLC), packed cell volume (PCV), and hemoglobin (Hb)], as compared to the low- and mid-dose (6-MP-CNPs) and saline treatment (Table 1). These toxic reductions could be because of an immunosuppressant activity of 6-MP. At the same time, the serum biochemical parameters [alanine aminotransferase (ALT), aspartate aminotransferase (AST), alkaline phosphatase (ALP), creatinine, and blood urea nitrogen (BUN)]were significantly ($^{ab}p < 0.001$) increased at high dose treatment of 6-MP and 6-MP-CNPs (Table 1). Likewise, these changes were in a dose-dependent manner. Based on our data and existing information, 6-MP is well-known to cause a significant toxic effect on bone marrow, liver, and kidney with reduced appetite, body weight (data not shown), and dehydration. These toxic consequences alter normal physiological profiles (Clarke et al., 1953; Philips et al., 1954). At low doses, all the haemato-biochemical parameters fell within the normal physiological range and were statistically significant ($^{ab}p < 0.001$) with the saline treatment group.

3.2.2.2. Histopathology. The H&E staining of the liver and kidney tissues are depicted in Fig. 4. The high dose of 6-MP treatment showed severe congestion in the central vein and sinusoidal space. The lesions of swollen hepatocytes with moderate vacuolization of cytoplasm and pyknotic nuclei were significant (Fig. 4). Pharmacologically, 6-MP metabolized into the active 6-TGN by hypoxanthine-guanine phosphoribosyltransferase (HGPRT). However, the catabolic conversions of 6-MP by thiopurine s-methyltransferase (TPMT) drive into the 6-methyl mercaptopurine and 6-methyl mercaptopurine ribonucleotides (6-MMP), which in turn, leads to hepatotoxicity (van Asseldonk et al., 2012; Zimm et al., 1985). We assume that the mid and high dose 6-MP-CNPswith its sustained release mechanism and altered catabolic process reduced the hepatic congestion and sinusoidal space with pyknotic nuclei (Fig. 4). Interestingly, no appreciable changes were noticed at the low dose of 6-MP-CNPs. At a high dose, the renal architecture showed severe congestion, tubular epithelial degeneration, and glomerular atrophy in 6-MP treatment as compared to 6-MP-CNPs (Fig. 4). These renal architectural changes might be as a result of an accumulation of 6-MP urinary metabolites in renal tubules, which can cause internal hydronephrosis (Oikonomou et al., 2011; Philips et al., 1954; Zimm et al., 1985). However, the low dose of 6-MP-CNPs showed no appreciable changes in renal architecture, whereas mild tubular epithelial degeneration with glomerular atrophy was observed for mid and high doses (Fig. 4).

4. Conclusion

Chitosan is a natural polysaccharide used to synthesise6-MP-CNPs as a novel drug-delivery system to reduce toxicity. The physicochemical interaction of chitosan and 6-MP was described using DLS, SEM, FTIR, and DSC. The loading efficiency of 6-MP in CNPs was estimated using LCMS/MS. Acute and subacute toxicity of 6MP-CNPs (vs 6-MP) shows reduced lethality (LD50) and has adverse effects on blood, liver, and renal profiles. Overall, the findings of this study suggest the importance of 6MP-CNPs as a drug-delivery system to reduce toxic profile and to improve therapeutic dosage in the *in vivo* preclinical studies.

Authorship contribution

All the authors contributed to this study. P.K.G., A.R.P., H.L.R., and J.S.S., hypothesized the project and study design. P.K.G., A.R.P., and J.S.S. performed the experiments. P.K.G., D.J., and H.L.R., analyzed the data and interpreted the results. P.K.G. wrote the manuscript draft. A.R.P., D.J., and H.L.R., read themanuscript and provided critical evaluation and theoretical insights. All the authors discussed and interpreted the results. All the authors read and approved the final version of the manuscript.

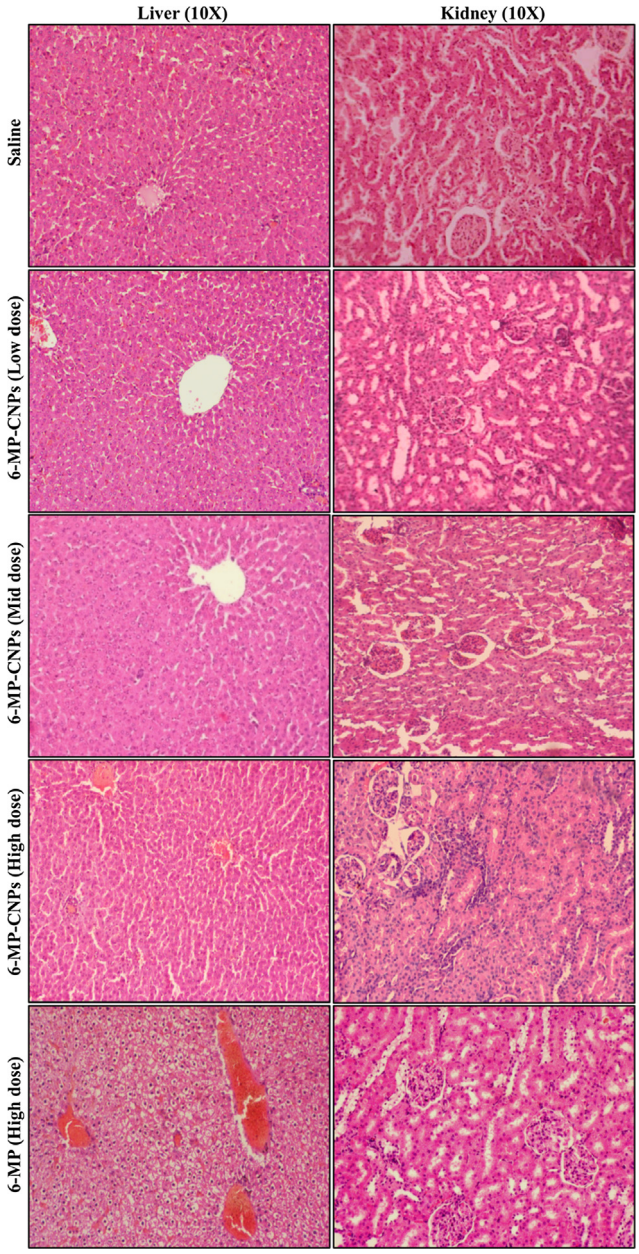

Fig. 4. Representative image of histopathological evaluation (H&E) of liver and kidney after 28-day repeated oral dosing of saline (2 mL/kg), 6-MP (50 mg/kg), and 6-MP-CNPs (low dose-15 mg/kg, mid dose-30 mg/kg, and high dose-50 mg/kg), n = 6, male.

Declaration of Competing Interest

The authors declare that they have no conflict of interest.

Acknowledgements

The authors are thankful to the management of the Department of Pharmacology and Toxicology, Veterinary College and Innovative Nano & Micro Technologies Private Limited (INM Technologies), Bangalore, Karnataka, India for providing the facilities and financial support to carry this investigation.

References

Adam de Beaumais, T., Fakhoury, M., Medard, Y., Azougagh, S., Zhang, D., Yakouben, K., Jacqz-Aigrain, E., 2011. Determinants of mercaptopurine toxicity in pediatric acute lymphoblastic leukemia maintenance therapy. Br. J. Clin. Pharmacol. 71, 575–584. https://doi.org/10.1111/j.1365-2125.2010.03867.x.

Agnihotri, S.A., Mallikarjuna, N.N., Aminabhavi, T.M., 2004. Recent advances on chitosan-based micro- and nanoparticles in drug delivery. J. Control. Release 100, 5–28. https://doi.org/10.1016/j.jconrel.2004.08.010.

Atyabi, F., Talaie, F., Dinarvand, R., 2009. Thiolated chitosan nanoparticles as an oral delivery system for Amikacin: in vitro and ex vivo evaluations. J. Nanosci. Nanotechnol. 9, 4593–4603.

Benkov, K., Lu, Y., Patel, A., Rahhal, R., Russell, G., Teitelbaum, J., Naspghan Committee on Inflammatory Bowel Disease, 2013. Role of thiopurine metabolite testing and thiopurine methyltransferase determination in pediatric IBD. J. Pediatr. Gastroenterol. Nutr. 56, 333–340. https://doi.org/10.1097/MPG.0b013e3182844705.

Berger, J., Reist, M., Mayer, J.M., Felt, O., Peppas, N.A., Gurny, R., 2004. Structure and interactions in covalently and ionically crosslinked chitosan hydrogels for biomedical applications. Eur. J. Pharm. Biopharm. 57, 19–34.

Clarke, D.A., Philips, F.S., Sternberg, S.S., Stock, C.C., Elion, G.B., Hitchings, G.H., 1953. 6-Mercaptopurine: effects in mouse sarcoma 180 and in normal animals. Cancer Res. 13, 593–604.

Coelho, T., Andreoletti, G., Ashton, J.J., Batra, A., Afzal, N.A., Gao, Y., Williams, A.P., Beattie, R.M., Ennis, S., 2016. Genes implicated in thiopurine-induced toxicity: Comparing TPMT enzyme activity with clinical phenotype and exome data in a pediatric IBD cohort. Sci. Rep. 6, 34658. https://doi.org/10.1038/srep34658.

Debnath, S.K., Saisivam, S., Debanth, M., Omri, A., 2018. Development and evaluation of Chitosan nanoparticles based dry powder inhalation formulations of Prothionamide. PLoS One 13, e0190976. https://doi.org/10.1371/journal.pone.0190976.

Dorniani, D., Hussein, M.Z.B., Kura, A.U., Fakurazi, S., Shaari, A.H., Ahmad, Z., 2013. Preparation and characterization of 6-mercaptopurine-coated magnetite nanoparticles as a drug delivery system. Drug Des. Devel. Ther. 7, 1015–1026. https://doi.org/10.2147/DDDT.S43035.

El-Shabouri, M.H., 2002. Positively charged nanoparticles for improving the oral bioavailability of cyclosporin-A. Int. J. Pharm. 249, 101–108.

Ferrero, F., Periolatto, M., 2012. Antimicrobial finish of textiles by chitosan UV-curing. J. Nanosci. Nanotechnol. 12, 4803–4810. https://doi.org/10.1166/jnn.2012.4902.

Fotoohi, A.K., Coulthard, S.A., Albertioni, F., 2010. Thiopurines: factors influencing toxicity and response. Biochem. Pharmacol. 79, 1211–1220. https://doi.org/10.1016/j.bcp.2010.01.006.

Gan, Q., Wang, T., 2007. Chitosan nanoparticle as protein delivery carrier–systematic examination of fabrication conditions for efficient loading and release. Colloids Surf B Biointerfaces 59, 24–34. https://doi.org/10.1016/j.colsurfb.2007.04.009.

Kumar, G.P., Phani, A.R., Prasad, R.G.S.V., Sanganal, J.S., Manali, N., Gupta, R., Rashmi, N., Prabhakara, G.S., Salins, C.P., Sandeep, K., Raju, D.B., 2014. Polyvinylpyrrolidone oral films of enrofloxacin: film characterization and drug release. Int. J. Pharm. 471, 146–152. https://doi.org/10.1016/j.ijpharm.2014.05.033.

Kumar, G.P., Sanganal, J.S., Phani, A.R., Manohara, C., Tripathi, S.M., Raghavendra, H. L., Janardhana, P.B., Amaresha, S., Swamy, K.B., Prasad, R.G.S.V., 2015. Anti-cancerous efficacy and pharmacokinetics of 6-mercaptopurine loaded chitosan nanoparticles. Pharmacol. Res. 100, 47–57. https://doi.org/10.1016/j.phrs.2015.07.025.

Lennard, L., Davies, H.A., Lilleyman, J.S., 1993. Is 6-thioguanine more appropriate than 6-mercaptopurine for children with acute lymphoblastic leukaemia?. Br. J. Cancer 68, 186–190.

Lv, X., Zhao, M., Wang, Y., Hu, X., Wu, J., Jiang, X., Li, S., Cui, C., Peng, S., 2016. Loading cisplatin onto 6-mercaptopurine covalently modified MSNS: a nanomedicine strategy to improve the outcome of cisplatin therapy. Drug Des Devel Ther 10, 3933–3946. https://doi.org/10.2147/DDDT.S116286.

Mohammed, M.A., Syeda, J.T.M., Wasan, K.M., Wasan, E.K., 2017. An overview of chitosan nanoparticles and its application in non-parenteral drug delivery. Pharmaceutics 9. https://doi.org/10.3390/pharmaceutics9040053.

Moll, F., 1971. Infrared spectroscopy of drugs. Fundamentals, methods and application. Mitt Dtsch. Pharm. Ges Pharm. Ges. DDR 41, 119–136.

National Research Council (US) Committee for the Update of the Guide for the Care and Use of Laboratory Animals, 2011. Guide for the Care and Use of Laboratory Animals, 8th ed, The National Academies Collection: Reports funded by National Institutes of Health. National Academies Press (US), Washington (DC).

Oikonomou, K.A., Kapsoritakis, A.N., Stefanidis, I., Potamianos, S.P., 2011. Drug-induced nephrotoxicity in inflammatory bowel disease. Nephron Clin. Pract. 119, c89–c94. https://doi.org/10.1159/000326682. discussion c96.

Peniche, C., Argüelles-Monal, W., Davidenko, N., Sastre, R., Gallardo, A., San Román, J., 1999. Self-curing membranes of chitosan/PAA IPNs obtained by radical polymerization: preparation, characterization and interpolymer complexation. Biomaterials 20, 1869–1878.

Philips, F.S., Sternberg, S.S., Hamilton, S., Clarke, D.A., 1954. The toxic effects of 6-mercaptopurine and related compounds. Ann. N. Y. Acad. Sci. 60, 283–296. https://doi.org/10.1111/j.1749-6632.1954.tb40019.x.

Sajeesh, S., Sharma, C.P., 2006. Novel pH responsive polymethacrylic acid-chitosan-polyethylene glycol nanoparticles for oral peptide delivery. J. Biomed. Mater. Res. Part B Appl. Biomater. 76, 298–305. https://doi.org/10.1002/jbm.b.30372.

Shu, X.Z., Zhu, K.J., 2002. The influence of multivalent phosphate structure on the properties of ionically cross-linked chitosan films for controlled drug release. Eur. J. Pharm. Biopharm. 54, 235–243.

Songjiang, Z., Lixiang, W., 2009. Amyloid-beta associated with chitosan nano-carrier has favorable immunogenicity and permeates the BBB. AAPS PharmSciTech 10, 900–905. https://doi.org/10.1208/s12249-009-9279-1.

Tamer, T.M., Hassan, M.A., Omer, A.M., Valachová, K., Eldin, M.S.M., Collins, M.N., Šoltés, L., 2017. Antibacterial and antioxidative activity of O-amine functionalized chitosan. Carbohydr. Polym. 169, 441–450. https://doi.org/10.1016/j.carbpol.2017.04.027.

Tang, Z.-X., Qian, J.-Q., Shi, L.-E., 2007. Preparation of chitosan nanoparticles as carrier for immobilized enzyme. Appl. Biochem. Biotechnol. 136, 77–96.

Tokumitsu, H., Ichikawa, H., Fukumori, Y., 1999. Chitosan-gadopentetic acid complex nanoparticles for gadolinium neutron-capture therapy of cancer: preparation by novel emulsion-droplet coalescence technique and characterization. Pharm. Res. 16, 1830–1835.

van Asseldonk, D.P., Seinen, M.L., de Boer, N.K.H., van Bodegraven, A.A., Mulder, C.J., 2012. Hepatotoxicity associated with 6-methyl mercaptopurine formation during azathioprine and 6-mercaptopurine therapy does not occur on the short-term during 6-thioguanine therapy in IBD treatment. J. Crohns. Colitis. 6, 95–101. https://doi.org/10.1016/j.crohns.2011.07.009.

Vora, A., Mitchell, C.D., Lennard, L., Eden, T.O.B., Kinsey, S.E., Lilleyman, J., Richards, S.M., Medical Research Council, National Cancer Research Network Childhood Leukaemia Working Party, 006. Toxicity and efficacy of 6-thioguanine versus 6-mercaptopurine in childhood lymphoblastic leukaemia: a randomised trial. Lancet 368, 1339–1348. https://doi.org/10.1016/S0140-6736(06)69558-5.

Walke, S., Srivastava, G., Nikalje, M., Doshi, J., Kumar, R., Ravetkar, S., Doshi, P., 2015. Fabrication of chitosan microspheres using vanillin/TPP dual crosslinkers for protein antigens encapsulation. Carbohydr. Polym. 128, 188–198. https://doi.org/10.1016/j.carbpol.2015.04.020.

Xu, Y., Du, Y., 2003. Effect of molecular structure of chitosan on protein delivery properties of chitosan nanoparticles. Int. J. Pharm. 250, 215–226.

Yeh, M., Cheng, K., Hu, C., Huang, Y., Young, J., 2011. Novel protein-loaded chondroitin sulfate-chitosan nanoparticles: preparation and characterization. Acta Biomater. 7, 3804–3812. https://doi.org/10.1016/j.actbio.2011.06.026.

Zimm, S., Ettinger, L.J., Holcenberg, J.S., Kamen, B.A., Vietti, T.J., Belasco, J., Cogliano-Shutta, N., Balis, F., Lavi, L.E., Collins, J.M., 1985. Phase I and clinical pharmacological study of mercaptopurine administered as a prolonged intravenous infusion. Cancer Res. 45, 1869–1873.